International Journal of Ambient Energy, 2013
http://dx.doi.org/10.1080/01430750.2012.759148

Taylor & Francis
Taylor & Francis Group

Modelling and simulation of a bio-fuelled conventional engine

B.P. Singh[a*] and P.K. Sahoo[b]

[a]*Moradabad Institute of Technology-244001, India;* [b]*College of Engineering Studies, University of Petroleum and Energy Studies, Dehradun, Uttarakhand, India*

(*Received 29 December 2011; final version received 18 October 2012*)

In the present work, a simulation model based on two different zones of combustion in compression ignition (CI) engines has been modified to predict the performance of a four-stroke CI engine. The modified model for the calculation of closed cycle of a four-stroke diesel engine is presented and applied for its operation with vegetable oil (Jatropha), which is considered as promising bio-fuels now a days. For the local temperature and cylinder pressure calculations, the mass and state equations are applied in each zone. The effect of fuel injection pressure and advance angle of fuel injection point on the brake thermal efficiency, brake-specific fuel consumption and nitric oxide emission has been analysed. The results from a computer program are compared and verified with the corresponding measurements from an experimental investigation conducted on the test bed. A good synchronisation is observed between the model's prediction and the available theoretical and experimental results. Engineering equation solver has been used as the programming input to the model.

Keywords: diesel engine; thermodynamic modelling; engine performance and emissions; Jatropha straight vegetable oil; engineering equation solver

1. Introduction

Several experimental studies have shown that vegetable oils can be used as an alternative fuel for diesel engines. Some of these vegetable oils are sunflower, rapeseed, cottonseed, jojoba and *Jatropha curcas*. Researchers have experimentally evaluated the performance characteristics of conventional diesel engines fuelled by bio-fuels and their blends. However, experiments require enormous effort, money and time. A realistic numerical simulation model could reduce such an effort. Numerical simulation based on mathematical modelling of diesel engine processes has been used as an aid by design engineers to develop new designs. However, with bio-fuel, only few works have been done and it is still a new area of research.

The process of diesel combustion is complex and heterogeneous in nature. Diesel engine combustion models are mainly described as thermodynamic and fluid dynamic models. Models based on thermodynamics can be further classified as single-zone heat release model, phenomenological jet-based model and quasi-dimensional multi-zone model. Single-zone models assume that the cylinder content is uniform in 'composition and temperature', and are suitable for the prediction of engine performance. Phenomenological combustion models are based on each individual processes occurring in engine cycle such as fuel injection, mixture formation, heat release, heat transfer and emission formation. Quasi-dimensional multi-zone models incorporate the development of the fuel spray with time and simplified quasi-steady equations are used to describe processes such as fuel injection, atomisation, air entrainment, droplet formation, evaporation, wall impingement, ignition, heat release, heat transfer, etc. Fluid dynamic-based models, often called multi-dimensional or computational fluid dynamics models, are based on solving the governing equations for conservation of mass, momentum and energy and species concentration through a definite discretisation procedure. Rakopoulos et al. (1995) developed a multi-zone model of a diesel engine cycle in order to examine the influence of insulating the combustion chamber on the performance and exhaust pollutants emissions of a naturally aspirated, direct injection, four-stroke and water-cooled diesel engine. They found that there is no remarkable improvement of engine efficiency, since the decrease in volumetric efficiency had a greater influence on it than the decrease in heat loss to the coolant, which was converted mainly to exhaust gas enthalpy (significant increase in the exhaust gas temperature). Zweiri, Whidborne, and Seneviratne (2001) developed an analytical non-linear dynamic model for single-cylinder diesel engines. The model described the dynamic behaviour between fuelling and engine speed and included models of the non-linear engine and dynamometer dynamics, the instantaneous friction terms and the engine thermodynamics. Quintero et al. (2007) presented a model for the calculation of in-cylinder parameters in an internal combustion engine with a noncircular gear-based modified

*Corresponding author. Email: bhanupratapmit@gmail.com

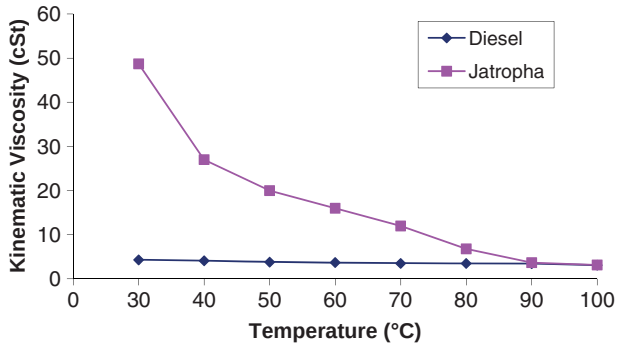

Figure 1. Variation of viscosity with temperature.

crank-slider mechanism. With the introduction of noncircular gears, the instantaneous velocity of the piston can be accommodated to improve combustion performance. Ganapathy, Murugesan, and Gakkhar (2009) proposed a methodology for the thermodynamic model analysis of Jatropha biodiesel engine in combination with Taguchi's optimisation approach to determine the optimum engine design and operating parameters.

2. Methodology

The combustion process can be described with varying complexities and accuracies.

Normally, the degree of complexity is decided by the number of zones in which the cylinder has been divided. An engine model therefore is either single-zone or multi-zone. In a single-zone model, the gas mixture within the cylinder is considered to be homogeneous for each sample. It is also assumed to be strictly made up of ideal gases. In a multi-zone model, for example, for a two-zone model, the gases are still considered ideal. However, the homogeneous approach has been replaced by a heterogeneous one. Here, the cylinder is also divided into two zones, one containing the injected fuel and the other surrounding air. Each zone is itself homogeneous and no heat transfer occurs between the two zones. The simplicity of the single-zone model is its favourable advantage. This makes it fast and therefore applicable in real-time systems. The multi-zone model is more complex and more accurate compared with the single-zone model. A multi-zone model is often needed for the combustion chamber design, but for most aspects of control design, a two-zone model is good enough. The brief overall structure of the methodology is shown in Figure 2.

3. The model

Due to the complexity of the diesel engine combustion and the turbulent fuel air-mixing, it is difficult to develop an effective model that does not take too long computational time. There are different approaches to implement a diesel combustion model, i.e. single-zone or multi-zone (Gogai and Baruch 2010; Rakopoulos, Antonopoulos, and Rakopoulos 2007). This has an acceptable simulation time and has a complexity level that reflects the timeframe of this paper; a two-zone model has been selected. The model includes only those processes occurring during closed cycle, when all valves are closed. The compression phase begins at the point of closing of the inlet valve (IVC) and continues up

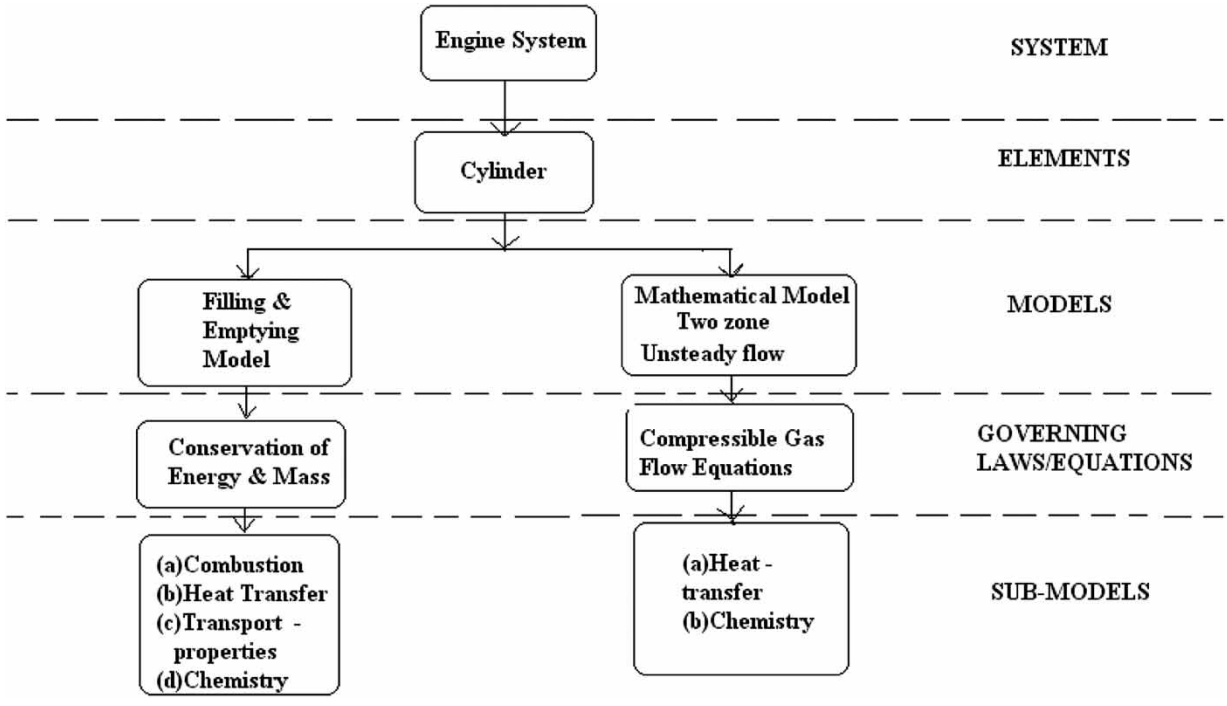

Figure 2. Overall structure of engine systems model.

to crank angle at which combustion begins. The period from the end of combustion to the exhaust valve opening (EVO) is the expansion phase. The compression and expansion phases are considered as polytrophic.

3.1. Energy balance equations

The energy balance equations for the present model can be expressed in a differential form. Then the first law of thermodynamics for compression phase, considering only one zone (pure air) is given as

$$\frac{\mathrm{d}Q}{\mathrm{d}\theta} = \frac{\mathrm{d}U}{\mathrm{d}\theta} + p\frac{\mathrm{d}V}{\mathrm{d}\theta}, \tag{1}$$

where $\mathrm{d}Q/\mathrm{d}\theta$ is the rate of heat loss to the combustion chamber walls, $\mathrm{d}U/\mathrm{d}\theta$ is the rate of change of internal energy and $p(\mathrm{d}V/\mathrm{d}\theta)$ is the rate of work done on the system.

During the combustion and expansion phases, at the start of combustion the entire volume is assumed to be the unburned region and at the end of combustion the entire volume is assumed to be the burned region. Therefore, the energy balance equation, using the two-zone model in the combustion chamber is given (Benson and Whitehouse 1979; Heywood 1998) and can be expressed by

$$m\frac{\mathrm{d}u}{\mathrm{d}\theta} + u\frac{\mathrm{d}m}{\mathrm{d}\theta} = \left(\frac{\mathrm{d}Qn}{\mathrm{d}\theta}\right) - \left(p\frac{\mathrm{d}V}{\mathrm{d}\theta}\right) - \left(\frac{30m_l h_l}{\pi N}\right). \tag{2}$$

All terms of the equation are elaborated as $\mathrm{d}u/\mathrm{d}\theta$ is the rate of change of internal energy of the mixture of mass m, $\mathrm{d}m/\mathrm{d}\theta$ is the rate of change of mixture mass m, $\mathrm{d}Q_n/\mathrm{d}\theta$ is the net heat release rate which is the difference between the rate of heat release during the combustion period and rate of heat transfer from combustion chamber gases to the combustion chamber walls, $p(\mathrm{d}V/\mathrm{d}\theta)$ is the rate of work done by the system.

Here, m is the mass of the mixture (air + fuel) contained in the combustion chamber (kg s), m_l is the mixture mass loss through piston rings (kg/s), h_l is the enthalpy loss (J/kg), N is the engine speed (rpm), θ is the crank angle (degree), V is the instantaneous cylinder volume (m^3), P is the cylinder pressure (Pa) and Q is the heat energy (J).

3.2. Volume at any crank angle

The instantaneous cylinder volume V_θ is given by

$$V_\theta = V_\mathrm{c} + \left\{\pi\frac{d^2}{4}\frac{l}{2}\right\}\{1 + m - (m^2 - \sin^2\theta)^{0.5} - \cos\theta\}, \tag{3}$$

where $m = (2.L).l^{-1}$, d is the cylinder bore (m), L is the connecting rod length (m), l is the stroke length (m), V_θ is the volume at any crank angle (m^3), V_c is the clearance volume (m^3) and θ is the crank angle.

3.3. Gas properties calculation

The gas properties are functions of pressure, temperature and its composition. Higher temperatures can be achieved for a system where the combustion is completed and the system becomes adiabatic. It depends on the chemical composition of the reactant mixture, pressure and temperature of the mixture and combustion process. A hydrocarbon fuel can be represented as $\mathrm{C}_x\mathrm{H}_y\mathrm{O}_z$. The chemically suitable amount of oxygen (O_cc) required for combustion per mole of fuel can be written as

$$O_\mathrm{cc} = m_\mathrm{c} + 0.25m_\mathrm{h} - 0.5m_\mathrm{o}. \tag{4}$$

The minimum amount of oxygen required (O_min) for combustion in the reactants per mole of fuel (to convert H_2 to H_2O and C to CO) can be expressed as

$$O_\mathrm{min} = O_\mathrm{cc} - 0.5m_\mathrm{c}. \tag{5}$$

Here, m_c, m_h and m_o are, respectively, the number of moles of carbon, hydrogen and oxygen atoms in 1 mol of fuel. From these mole fraction calculations, mixture properties such as enthalpy, internal energy, specific volume and specific heat at constant pressure are calculated.

3.4. Internal energy

The internal energy (u) can be written in terms of the internal energy of unburned zone U_u and burned zone U_b with (x) as a mass fraction burned as

$$u = \frac{U}{m} = xU_\mathrm{b} + (1-x)U_\mathrm{u}. \tag{6}$$

Similarly, the specific volume can be written in terms of the specific volume of the unburned zone (u) and the burned zone (b) as

$$v = \frac{V}{m} = xv_\mathrm{b} + (1-x)v_\mathrm{u}. \tag{7}$$

Differentiating Equations (6) and (7) with respect to the crank angle and replacing the partial derivative terms with the logarithmic forms give the internal energy and specific volumes for the burnt and unburnt zones as

$$\left(\frac{\mathrm{d}v_\mathrm{b}}{\mathrm{d}\theta}\right) = \left(\frac{v_\mathrm{b}\partial(\ln v_\mathrm{b})\mathrm{d}T_\mathrm{b}}{T_\mathrm{b}\partial(\ln T_\mathrm{b})\mathrm{d}\theta}\right) + \left(\frac{v_\mathrm{b}\partial(\ln v_\mathrm{b})\mathrm{d}P}{P\partial(\ln P)\mathrm{d}\theta}\right), \tag{8}$$

$$\left(\frac{\mathrm{d}v_\mathrm{u}}{\mathrm{d}\theta}\right) = \left(\frac{v_\mathrm{u}\partial(\ln v_\mathrm{u})\mathrm{d}T_\mathrm{u}}{T_\mathrm{u}\partial(\ln T_\mathrm{u})\mathrm{d}\theta}\right) + \left(\frac{v_\mathrm{u}\partial(\ln v_\mathrm{u})\mathrm{d}P}{P\partial(\ln P)\mathrm{d}\theta}\right), \tag{9}$$

$$\left(\frac{\mathrm{d}u_\mathrm{b}}{\mathrm{d}\theta}\right) = \left(C_{p\mathrm{b}} - \frac{Pv_\mathrm{b}\partial(\ln v_\mathrm{b})}{T_\mathrm{b}\partial(\ln T_\mathrm{b})}\right)\frac{\mathrm{d}T_\mathrm{b}}{\mathrm{d}\theta} - v_\mathrm{b}\left(\frac{\partial(\ln v_\mathrm{b})}{\partial(\ln T_\mathrm{b})} + \frac{\partial(\ln v_\mathrm{b})}{\partial(\ln P)}\right)\frac{\mathrm{d}P}{\mathrm{d}\theta}, \tag{10}$$

$$\left(\frac{\mathrm{d}u_\mathrm{u}}{\mathrm{d}\theta}\right) = \left(C_{p\mathrm{u}} - \frac{Pv_\mathrm{u}\partial(\ln v_\mathrm{u})}{T_\mathrm{u}\partial(\ln T_\mathrm{u})}\right)\frac{\mathrm{d}T_\mathrm{u}}{\mathrm{d}\theta} - v_\mathrm{u}\left(\frac{\partial(\ln v_\mathrm{u})}{\partial(\ln T_\mathrm{u})} + \frac{\partial(\ln v_\mathrm{u})}{\partial(\ln P)}\right)\frac{\mathrm{d}P}{\mathrm{d}\theta}, \tag{11}$$

where C_{pb} and C_{pu} are the specific heat capacity at constant pressure for the burned and unburned zones. Furthermore, the first term in Equation (2) can be written as follows:

$$\left(m\frac{\mathrm{d}u}{\mathrm{d}\theta}\right) = \left(x\frac{\mathrm{d}u_b}{\mathrm{d}\theta} + (1-x)\frac{\mathrm{d}u_u}{\mathrm{d}\theta} + (u_b - u_u)\frac{\mathrm{d}x}{\mathrm{d}\theta}\right)m, \tag{12}$$

where x is the mass burned fraction and can be calculated by the Weibe function by using the following expression (Heywood 1998):

$$x = 1 - \exp\left[-a\left(\frac{\theta-\theta_0}{\Delta\theta}\right)^{c+1}\right], \tag{13}$$

where θ_0 is the start of combustion and $\Delta\theta$ is the combustion duration and a is an adjustable parameter that characterises the completeness of the combustion process. The parameter c represents the rate of combustion. The value of c for all fuels is taken as 2.0 and a as 5.0 (Heywood 1998).

3.5. Heat loss from the combustion chamber

The heat loss from the combustion chamber can also be expressed by using both burned and unburned zones as follows:

$$\left(\frac{\mathrm{d}Q}{\mathrm{d}\theta}\right) = \left(\frac{30(Q_b + Q_u)}{\pi N}\right), \tag{14}$$

where

$$Q_b = hA_b(T_b - T_w), \tag{15}$$

$$Q_u = hA_u(T_u - T_w). \tag{16}$$

The surface areas of the two different zones are given by A_u and A_b. These areas can be related to a mass fraction burned x by using an empirical formula (Ferguson 1986):

$$A_b = \left(\frac{\pi d^2}{2} + \frac{4V}{d}\right)x^{0.5}, \tag{17}$$

$$A_u = \left[\left(\frac{\pi d^2}{2} + \frac{4V}{d}\right)(1 - x^{0.5})\right], \tag{18}$$

where d is the bore of the cylinder (m). The convective heat transfer coefficient h for Equations (15) and (16) is given by Prasath, Tamilporai, and Shabir Mohd (2010) as follows:

3.6. Heat transfer coefficient

Heat transfer coefficient of gas for each degree crank angle is calculated from the following equation as

$$h = 0.26\left(\frac{k}{d}\right)Re^{0.6}, \tag{19}$$

where k is the thermal conductivity for each change in viscosity (W/m k) and Re is the Reynolds number for each time step is calculated as follows:

$$Re = \frac{\rho \mathrm{d}V_p}{\mu}, \tag{20}$$

where ρ is the density of the gas mixture (kg/m^3), μ is the dynamic viscosity (kg/m s) and V_p is the mean piston speed (m/s).

3.7. Instantaneous pressure and temperature of unburned and burned zones of the combustion chamber

The instantaneous pressure and temperature for different zones at any crank angle can be calculated as

$$\left(\frac{\mathrm{d}P}{\mathrm{d}\theta}\right) = \left(\frac{A+B+C}{D+E}\right), \tag{21}$$

where terms A, B, C, D and E can be explained as

$$A = \frac{1}{m}\left(\frac{\mathrm{d}V}{\mathrm{d}\theta} + \frac{30VC_b}{\pi N}\right), \tag{21a}$$

$$B = h\left(\frac{30\left((\pi d^2/2) + (4V/d)\right)}{\pi Nm}\right) \times \left(\frac{v_b \partial \ln v_b}{C_{pb}\partial \ln T_b}x^{1/2}\frac{T_b - T_w}{T_b} + \frac{v_u \partial \ln v_u}{C_{pu}\partial \ln T_u}(1 - x^{1/2})\frac{T_u - T_w}{T_u}\right), \tag{21b}$$

$$C = -(v_b - v_u)\frac{\mathrm{d}x}{\mathrm{d}\theta} - v_b\frac{\partial \ln v_b}{\partial \ln T_b}\frac{h_u - h_b}{C_{pb}T_b} \times \left[\frac{\mathrm{d}x}{\mathrm{d}\theta} - \frac{(x - x^2)C_b 30}{\pi N}\right], \tag{21c}$$

$$D = x\left(\frac{v_b^2}{C_{pb}T_b}\left(\frac{\partial \ln v_b}{\partial \ln T_b}\right)^2 + \frac{v_b \partial \ln v_b}{P\partial \ln P}\right), \tag{21d}$$

$$E = (1-x)\left(\frac{v_u^2}{C_{pu}T_u}\left(\frac{\partial \ln v_u}{\partial \ln T_u}\right)2 + \frac{v_u}{P}\frac{\partial \ln v_u}{\partial \ln P}\right), \tag{21e}$$

$$\left(\frac{\mathrm{d}T_b}{\mathrm{d}\theta}\right) = \frac{-h\left((\pi d^2/2) + (4V/d)\right)x^{1/2}(T_b - T_w)30}{\pi NmC_{pb}x} + \left[\frac{v_b}{C_{pb}}\frac{\partial \ln v_b}{\partial \ln T_b}\left(\frac{A+B+C}{D+E}\right)\right] + \frac{h_u - h_b}{C_{pb}x}\left[\frac{\mathrm{d}x}{\mathrm{d}\theta} - \frac{(x-x^2)C_b 30}{\pi N}\right], \tag{22}$$

$$\left(\frac{\mathrm{d}T_u}{\mathrm{d}\theta}\right) = \frac{-30h\left(\frac{\pi d^2}{2} + \frac{4V}{d}\right)(1 - x^{1/2})(T_u - T_w)}{\pi NmC_{pu}(1-x)} + \left[\frac{v_u}{C_{pu}}\frac{\partial \ln v_u}{\partial \ln T_u}\left(\frac{A+B+C}{D+E}\right)\right], \tag{23}$$

where C_b is the blow by constant and h_l is the enthalpy loss which can be determined as

$$h_l = (1 - x^2)h_u + x^2 h_b. \quad (24)$$

3.8. Ignition delay

The ignition delay is the time duration between the start of fuel injection and the start of combustion. Many expressions for ignition delay are found in the literature as a function of mixture pressure, temperature; fuel cetane number (CN) (Bibic et al. 2008; Ramadhas, Jayaraj, and Muraleedharan 2006). The following empirical correlation is used to obtain the value of the ignition delay (Bibic et al. 2008; Ganesan 2000):

$$t_d = \frac{2.64}{P^{0.8}\phi^{0.2}} \exp\left(\frac{1650 - 20\text{CN}}{RT}\right), \quad (25)$$

where R is the universal gas constant and φ is the fuel air equivalence ratio. However, the constants and exponents in the above correlation are to be better calibrated against experimental results and conclusion.

3.9. Mass of fuel injected

Considering that the nozzle open area is constant during the injection period, the total mass of the fuel injected for each crank angle is calculated as follows:

$$m_f = C_d A_n \sqrt{2\rho_f \Delta P}\left(\frac{\Delta\theta_f}{360N}\right) n, \quad (26)$$

where n is the number of injector nozzle holes, C_d is the coefficient of discharge of injector nozzle, A_n is the cross-sectional area of nozzle (m^2), ΔP is the pressure drop in the nozzle (Pa), N is the engine speed and $\Delta\theta_f$ is the fuel injection period.

3.10. Pressure drop in the nozzle

The pressure drop in the nozzle is calculated as follows (Rakopoulos et al. 2004):

$$\Delta P = 0.5\rho_f \left(\frac{u_{inj}}{C_d}\right)^2, \quad (27)$$

where u_{inj} the spray velocity from the nozzle hole is given as

$$u_{inj} = \left(\frac{dm_f}{d\theta}\right)\left(\frac{6N}{\rho_f A n}\right), \quad (28)$$

where $dmf/d\theta$ is the fuel injection rate (kg/°CA).

$$\left(\frac{dm_f}{d\theta}\right) = \left(\frac{m_f}{n\Delta\theta_f}\right). \quad (29)$$

3.11. Sauter mean diameter

It is the ratio of mean volume to the mean surface area of the fuel droplets and has an important role in defining the fuel atomisation characteristics. Smaller sauter mean diameter (SMD) results in better fuel atomisation and ultimately better fuel combustion efficiency

$$\text{SMD} = 3.08\nu^{0.335}(\sigma\rho_f)^{0.737}\rho_a^{0.06}(\Delta P)^{-0.54}, \quad (30)$$

where ν is the kinematic viscosity (m^2/s, σ is the surface tension of the fuel (N/m), ρ_f is the density of the fuel (kg/m^3), ρ_a is the density of air (kg/m^3) and ΔP is the pressure drop across the nozzle (Pa).

3.12. Net work done

Work done in each crank angle is calculated from (Heywood 1998):

$$dW = \left(\frac{P_1 + P_2}{2}\right)(V_2 - V_1), \quad (31)$$

where P_1 and P_2 are the change in pressure for each crank angle inside the combustion chamber, and V_1 and V_2 are the changes in volume inside the combustion chamber for the same crank angle.

3.13. Nitric oxide formation

The consideration of chemical equilibrium cannot predict the actual nitric oxide (NO) concentration. The general accepted kinetics formation scheme proposed by Lavoie, Heywood, and Keck (1970) is used. The equations that describe the model together with their forward reaction rate constants k_{if} ($m^3/kmol/s$) are as follows:

$$\text{N} + \text{NO} \leftrightarrow \text{N}_2 + \text{O}, \quad k_{if} = 3.1 \times 10^{10} \exp^{(-160/T)}, \quad \text{(a)}$$

$$\text{N} + \text{O}_2 \leftrightarrow \text{NO} + \text{O}, \quad k_{2f} = 6.4 \times 10^{6} \exp^{(-3125/T)}, \quad \text{(b)}$$

$$\text{N} + \text{OH} \leftrightarrow \text{NO} + \text{H}, \quad k_{3f} = 4.2 \times 10^{10}. \quad \text{(c)}$$

The change of NO concentration (in $kmol/m^3$) is expressed as follows:

$$\frac{1}{V}\left(\frac{d((NO)V}{dt}\right) = 2(1 - \alpha^2)\left(\frac{R_1}{1 + \alpha R_1/(R_2 + R_3)}\right), \quad (32)$$

where R_i is the one-way equilibrium rate for reaction i, defined as

$$R_1 = k_{1f}(\text{N})_e(\text{NO})_e, \quad R_2 = k_{2f}(\text{N})_e(\text{O}_2)_e,$$
$$R_3 = k_{3f}(\text{N})_e(\text{OH})_e$$

with index 'e' denoting the equilibrium concentration and term $\alpha = (\text{NO})/(\text{NO})_e$.

4. Procedure for the numerical solution

The equations of the model adopted in the previous section are suitable for any hydrocarbon fuel as diesel, vegetable oil, biodiesel, etc. These equations are solved numerically using time step size of 2° crank angles. The input parameters used in the model are injection pressure, crank angle and the molecular formula of the diesel and Jatropha oil. The several physical and thermal properties are also used as input parameters as shown in Table 1. The outputs of the model programme are instantaneous pressure, temperature, volume and the performance parameters that include brake thermal efficiency (BTE), brake-specific fuel consumption (BSFC) and NO_x emission.

4.1. Numerical solution stages

In brief, the numerical solution stages consist of the calculation of compression phase, calculations of combustion and expansion phases and calculation of the air (unburned) and burning phase.

4.1.1. Computation of the compression phase

(i) Introduce the data at the IVC event, i.e. P_1, T_1, trapped composition (air with no fuel) and compute V_1 from engine geometry. Select the crank angle step size $\Delta\theta$, here to 2°.

(ii) The initial internal energy E_1 was calculated using its T_1 relation and similarly for the heat capacities C_p and C_v.

(iii) For the new crank angle $\theta_2 = \theta_1 + \Delta\theta$, compute V_2 from the engine geometry.

(iv) Temperature T_2 was estimated by assuming an isentropic change:

$$T_2 = T_1 * \left(\frac{V_1}{V_2}\right)^{(R/Cv*T_1)}.$$

Then, find pressure P_2 from the perfect gas state equation:

$$P_2 = \left(\frac{V_1}{V_2}\right) * \left(\frac{T_2}{T_1}\right) * P_1.$$

(v) The internal energy E_2 was calculated using its T_2 relation.

(vi) Calculate the work in the step:

$$\mathrm{d}W = \frac{P_1 + P_2}{2(V_2 - V_1)}.$$

(vii) Calculate $\mathrm{d}Q$ from the heat loss model.

(viii) Apply the first law of thermodynamics for a closed system.

$$f(E) = E_2 - E_1 + \mathrm{d}W - \mathrm{d}Q = 0.$$

Solve the equation with respect to T_2 using the Newton–Rapson numerical method so that a better estimate of T_2 is found.

(ix) Calculate P_2 for the revised value of T_2 using the gas state equation at the time moments 1 and 2.

(x) Repeat steps (v)–(ix) until the error $f(E)$ in the first law equation is negligible.

(xi) Continue this way, until θ_2 equals the value at the start of fuel injection.

4.1.2. Computation of combustion and expansion phase

(i) Connect the forming two-zone system with the previous single-zone one.

(ii) Set the conditions at the end of the previous time step (old state) as initial conditions for the current time step (new state) for both zones.

(iii) For crank angle $\theta_2 = \theta_1 + \Delta\theta$, compute V_2 from the engine geometry.

(iv) Estimate pressure p_2 at the end of the time step, to be checked later on, by assuming isentropic change (with $\gamma = 1.35$), $P_2 = P_1\ (V_1/V_2)^{\gamma}$.

(v) Check the temperatures of all zones.

(vi) Check the volumes of the zones and change pressure P_2 if necessary.

(vii) Calculate various useful quantities, such as the gross and net heat release rates as well as their cumulative values at each step.

(viii) Repeat steps (i)–(vii) and continue this way until $\Delta\theta$ reaches the EVO event, i.e. the end of the closed cycle.

4.1.3. Calculation for the unburned zone

The calculations in this zone were similar to the ones during the compression phase.

Table 1. Instruments to measure various properties and their values.

Property	Instrument	Measured and calculated value of diesel oil	Measured and calculated value of Jatropha oil
Density (kg/m^3)	Hydrometer	817	910
Kinematic viscosity at 70°C (cSt)	Rotational viscometer	3.5	12
Surface tension at 27°C (N/m)	Multi-frequency ultrasonic interferometer	0.028	0.042
Calorific value (MJ/kg)	Bomb calorimeter	43.04	37.08

(i) The initial internal energy E_1 was calculated using its T_{1u} relation and similarly for the enthalpy h_1 and heat capacity C_v (T_{1u}) of air.
(ii) V_{1u} was calculated from the gas state equation, $V_{1u} = (m\,\mathrm{R\,mol}\,T_{1u})/P_1$ where m was the total k mol in the air zone at state 1 per mol.
(iii) Make a first estimate of T_{2u} considering an isentropic change.
(iv) The internal energy E_2 was calculated using its T_{2u} relation and similarly for the heat capacity C_v (T_{2u}) of air.
(v) V_{2u} was calculated from the gas state equation, $V_{2u} = m\,\mathrm{R\,mol}\,T_{2u}/P_2$.
(vi) Calculate the work in the step, $\mathrm{d}W = 0.5(P_1 + P_2)\,(V_{2u} - V_{1u})$.
(vii) Apply the first law of thermodynamics for an open system. Solve the equation with respect to T_{2u} using the Newton–Rapson numerical method, so that a better estimate of T_{2u} is found.
(viii) Repeat steps (iv)–(vii) until the error f (E) in the first law equation is negligible.

4.1.4. *Calculation for burned zones*

(i) The internal energy of the burning zone was calculated at state 1 E_{1b}, from its T_{1b} relation.
(ii) Estimate the temperature T_{2b} at the end of the time step (state 2), i.e. after combustion, considering an isentropic change.
(iii) Estimate the volume of the burning zone using the gas state equation.
(iv) The internal energy E_{2b} was calculated using its T_{2b} relation and similarly for the heat capacity C_v (T_{2b}) in state 2.
(v) The volume in state 2 was calculated using the gas state equation.
(vi) Calculate the work $\mathrm{d}W_1$ in the time step, for a change from state 1 after mixing to state 2, $\mathrm{d}W_1 = 0.5(P_1 + P_2)(V_{2b} - V_{1b})$.
(vii) Apply the first law of thermodynamics for a change from state 1 to state 2 (a closed system is considered, since the addition of air has already been taken into account). Solve the equation with respect to T_{2b} using the Newton–Rapson numerical method, so that a better estimate of T_{2b} is found.
(viii) Repeat steps (iv)–(vii) until the error f (E) in the first law equation is negligible.
(ix) Compute the quantity of NO in the burning zone by solving the relevant differential equation.
(x) Finally, calculate the work for the total change from state 1 (unburned) to state 2, since this is the real work produced: $\mathrm{d}W = 0.5(P_1 + P_2)\,(V_{2b} - V_{1b})$.

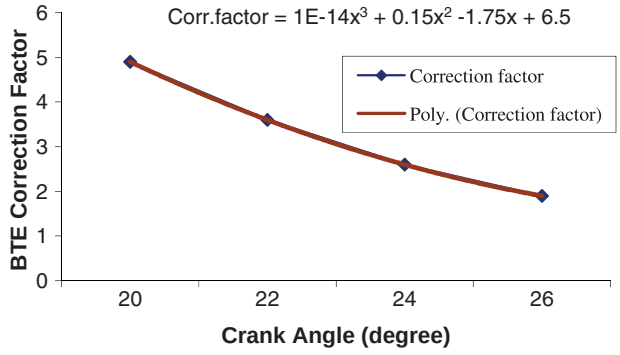

Figure 3. BTE correction factor with crank angle.

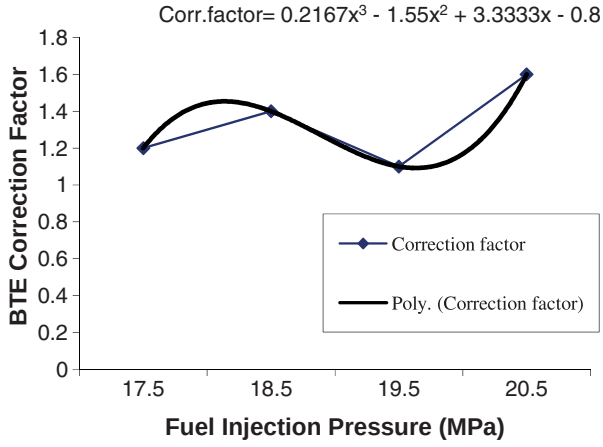

Figure 4. BTE correction factor with fuel injection pressure.

4.2. *Correction factor for various performances and emission parameters*

The correction factor for different performances and emission parameters can be determined by different governing equation as explained below. With the help of these equations, the correction factor can be calculated for any variable condition which are given in the form of the x-axis variable. After putting these variables in the correction factor equation, the value of the correction factor can be calculated for that performance and emission parameters. The calculated value for those parameters is added or subtracted in the calculated value of the modified model and the proposed value is obtained. Therefore, we can calculate the approximated value of the required parameters.

4.2.1. *Brake thermal efficiency*

The correction factor for BTE is explained in two variable conditions, namely first by varying the crank angle and second the fuel injection pressure. Figures 3 and 4 show the value of the correction factor in the form of the governing equation. The values of the correction factor in both conditions are found out by putting the crank angle and fuel injection pressure as input variables in the respective governing equations.

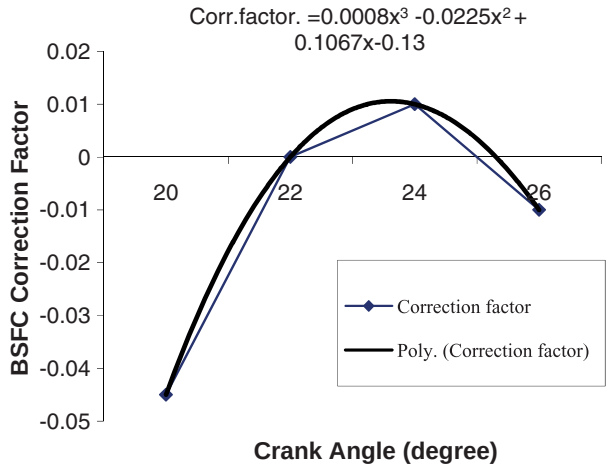

Figure 5. BSFC correction factor with crank angle.

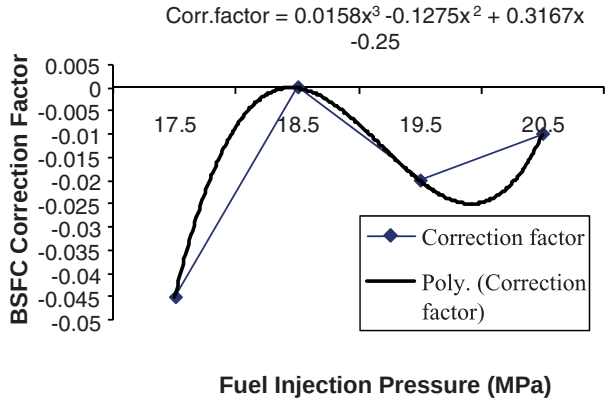

Figure 6. BSFC correction factor with fuel injection pressure.

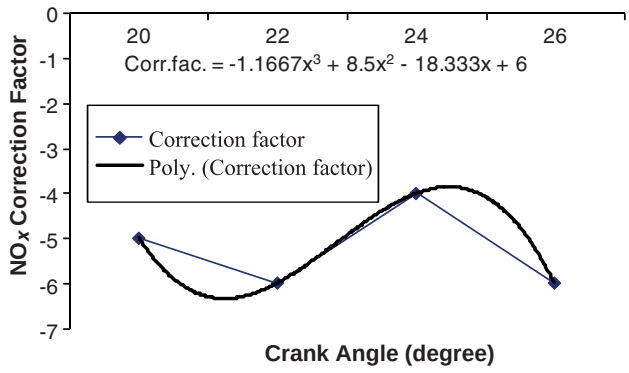

Figure 7. NO_x correction factor with crank angle.

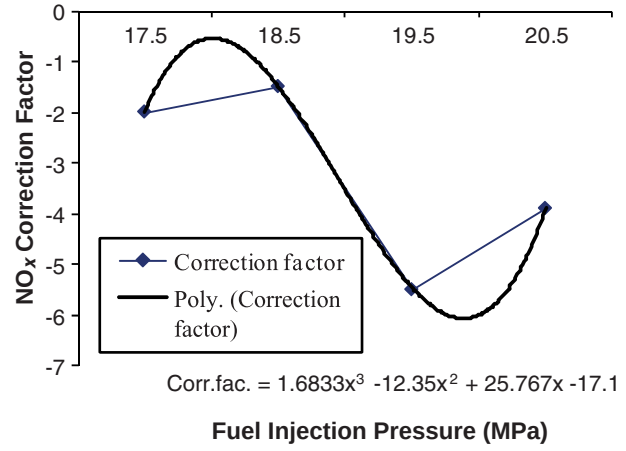

Figure 8. NO_x correction factor with fuel injection pressure.

4.2.2. *Brake-specific fuel consumption*

Figures 5 and 6 show the correction factor for BSFC variations with the crank angle and fuel injection pressure. Between the crank angles from 20° to 22°, the value of correction factor is negative. This is because of taking some assumptions in modelling with respect to actual conditions. Same trends also continue from 25° onwards. But in the case of varying fuel injection pressures all the values of correction factor are in the negative side. These are all due to setting the conditions at the end of the previous time step (old state) as initial conditions for the current time step (new state) for both zones and estimating pressure p_2 at the end of the time step, to be checked later on, by assuming isentropic change (with $\gamma = 1.35$), $P_2 = P_1\ (V_1/V_2)^{\gamma}$. However, in actual conditions these are not isentropic changes.

4.2.3. *NO_x emission*

NO_x correction factor variations with fuel injection pressure and crank angle are shown in Figures 7 and 8. In both the varying conditions, the values of correction factor are negative and mainly differ from the trends line. These are due to not correctly calculating the numbers of moles of each constituent which are taking part in combustions, which affects the gas properties' calculations.

4.3. *Effect of the density of air on the heat transfer per the crank angle*

The variations of heat transfer per crank angle with respect to density of air are shown in the Figure 9. As density of air increases in the combustion chamber, heat transfer also increases. So such types of variations of heat transfer and air density verify the programme developed.

4.4. *Net work done output with the crank angle*

The net work done with crank angle variations is shown in Figure 10. The negative work done in the figure shows that the work is done on the system in the compression phase, that is, from 225° to 345°. After the fuel injection into the combustion chamber, burning takes place. At this stage, the pressure rise in the cylinder takes place and the expansion phase starts which shows the positive work done.

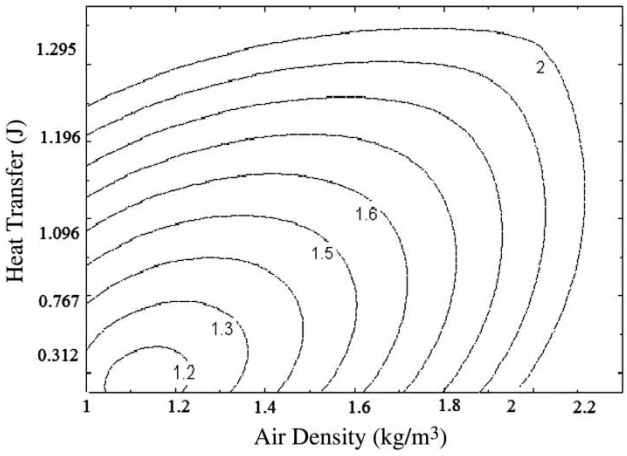

Figure 9. Variation of heat transfer per crank angle *vs*. density of air.

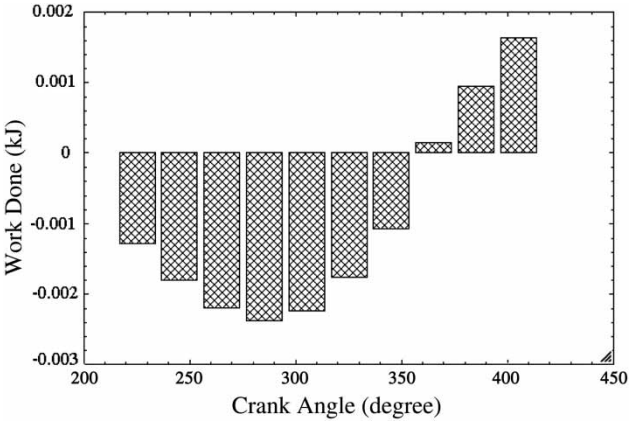

Figure 10. Variation of work done *vs*. crank angle.

5. Experimental analysis

In the present investigation, Jatropha oil, a non-edible type vegetable oil, is chosen as a potential alternative fuel and it is used as the fuel in compression ignition (CI) engines. The oil content of Jatropha seed ranges from 30% to 40% by weight and the kernel itself ranges from 45% to 60% (Pramanik 2003). Fresh Jatropha oil is slow-drying, odourless and colourless oil, but it turns yellow after ageing. Some of the properties of Jatropha oil fall within a fairly narrow band and are quite close to those of the diesel oil. The main problem of using Jatropha oil in unmodified form in diesel engine is its high viscosity. Therefore, it is necessary to reduce the fuel viscosity before injecting it in the engine. High viscosity of Jatropha oil can be reduced by heating the oil using waste heat of exhaust gases from the engine. The various procedures followed and the instruments used are given in Table 1. The viscosity of Jatropha oil and diesel was measured at different temperatures to find the effect of temperature on viscosity (Figure 1).

The engine selected for the present study is widely used, mostly for agricultural irrigational purposes and also in many other small- and medium-scale commercial applications such as producing electricity, running flour mills, rice mills. A single-cylinder, four-stroke, vertical, water-cooled, indirect injection diesel engine was selected for the experiments. The technical specifications of the engines are given in Table 2. The engine can be started by hand cranking using the decompression lever. The test engine is coupled with a single-phase, 230 V AC alternator of 7.5 kVA capacities to absorb the maximum power produced by the engine.

Table 2. Tested engine specifications.

Manufacturer	Field Marshal Engine Ltd., India
Model	FM-4
Engine type	Vertical, four-stroke, single-cylinder, CI engine
Rated power	7.35 kW at 1000 rpm
Bore/stroke	120/139.7 (mm)
Compression ratio	17:1
Nozzle	DL30S12002MICO
Nozzle holder	9430031264MICO
Fuel pump plunger	9 × 03/323MICO
Nozzle opening pressure	145 bar
Sump capacity	4.5 l

Table 3. Chemical name and formula of some common fatty acids (Balat and Balat 2008).

Name of the fatty acid	Chemical name of fatty acid	Formula
Lauric	Dodecanoic	$C_{12}H_{24}O_2$
Myristic	Tetradecanoic	$C_{14}H_{28}O_2$
Palmitic	Hexadecanoic	$C_{16}H_{32}O_2$
Stearic	Octadecanoic	$C_{18}H_{36}O_2$
Oleic	*cis*-9-Octadecanoic	$C_{18}H_{34}O_2$
Linoleic	*cis*-9, *cis*-12-Octadecadienoic	$C_{18}H_{32}O_2$

6. Results and discussions

In the combustion modelling, the molecular formula of the diesel fuel is taken as $C_{10}H_{22}$. From the fatty acid composition, Jatropha is classified as linoleic or oleic acid types, which are unsaturated fatty acids (Pramanik 2003). So based on these properties, the molecular formula of Jatropha oil is approximated as $C_{18}H_{32}O_2$ (Balat and Balat 2008; Barnwal and Sharma 2005). In general, this combustion model, developed for the CI engine analysis, is suitable for any hydrocarbon fuel. This includes diesel, biodiesel or their blends as well as vegetables oil. The engine model is analysed for the variation in fuel injection pressure, point of fuel injection and fuel inlet temperature for the diesel as well as Jatropha oil (Table 3).

6.1. Effect of fuel injection point on BTE

The fuel injection point is taken for the analysis because the time duration between the point of fuel injection and the start

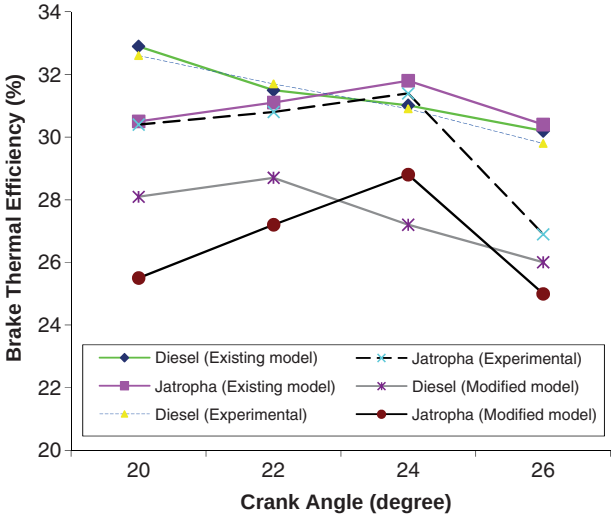

Figure 11. BTE *vs*. crank angle (BTDC) at speed 1000 rpm, 80% of full load and static 175 bar injection pressure.

of combustion process has been felt to be one factor which is not sufficient to allow the fuel particles to get atomised properly. The increase in time delay provides more time available for this pre-combustion. It is stated that Jatropha oil requires higher ignition timing for better combustion and hence improves the engine performance and emission characteristics (Banapurmath, Tewari, and Hosmath 2008). Advancing the fuel injection point by 1° results in an increase in ignition delay of 0.07 s. This results in better fuel atomisation characteristics and enhances the combustion efficiency. The increase in delay period is achieved by advancing the fuel injection point. In the present model, reference or static point of fuel injection is taken 20° before top dead centre (BTDC) for the diesel fuel. The fuel injection point used for the analysis of model is 20° BTDC to 26° BTDC in 2° steps. Advancing the fuel injection point is limited because increased delay period increases the possibility of engine detonation and affects efficiency. The possible reason for detonation and reduction in engine performance is due to the fact that advanced ignition timing results in an increased peak pressure and temperature before and around the TDC.

Figure 11 represents the variation of BTE as a function of crank angle at speed 1000 rpm and 80% of full load (7.35 kW) for different modelling and experimental conditions. BTE decreases with advancing crank angle for diesel fuel. But in the case of Jatropha oil, it first increases up to 24° and then started decreasing. Due to the increased brake power and less fuel energy input with Jatropha oil, the BTE trend increases in the case of Jatropha oil. But it starts to decrease as injection timing is more advanced, as cylinder pressure and temperature during the delay period become lower. Therefore, the ignition delay period becomes longer (Senthil Kumar, Ramesh, and Nagalingam 2003). This phenomenon results in more fuel being burnt during the premixed combustion phase following the ignition delay period.

6.2. *Effect of fuel injection pressure on BTE*

The effect of varying fuel injection pressures at a constant fuel injection point has been investigated in the model at different pressures from 175 to 205 bar in 10 bar step variation. The investigation has been carried out with the objective of the fuel atomisation characteristics that indirectly depend upon fuel droplet size injected into the combustion chamber (as the droplet size reduces at high fuel injection pressure). The SMD has an important role in defining the fuel atomisation characteristics. Smaller SMD results in better fuel atomisation and ultimately the fuel combustion efficiency. The SMD of diesel at room temperature and an injection pressure of 175 bar is found to be 3.82×10^{-5} m. The SMD of diesel can be reduced from 3.82×10^{-5} to 3.5×10^{-5} m as the pressure increases from 175 to 205 bar. The SMD of Jatropha oil at room temperature and 175 bar is obtained as 12.56×10^{-5} m. It reduces from 12.56×10^{-5} to 11.53×10^{-5} m as the pressure is increased from 175 to 205 bar. As Jatropha oil is heated up to 90°C, the SMD at 175 bar can be reduced from 12.56×10^{-5} to 4.33×10^{-5} m. This is a substantial reduction in SMD by preheating. Preheating the fuel has lowered the viscosity from 48.7×10^{-6} to 3.68×10^{-6} m^2/s. The comparison of SMD for Jatropha oil and diesel at room temperature showed that the difference between them is very high 8.74×10^{-5} m. This difference can be reduced to a good extent (0.5×10^{-5} m) as the Jatropha oil is preheated. This appreciable improvement is due to the fact that the viscosity and surface tension reduces to a sufficiently high extent. Figure 12 represents the behaviour of BTE as a function of the fuel injection pressure at a constant speed, load and point of injection for different modelling and experimental conditions. BTE decreases as fuel injection pressure either decreases or increases from 195 bar.

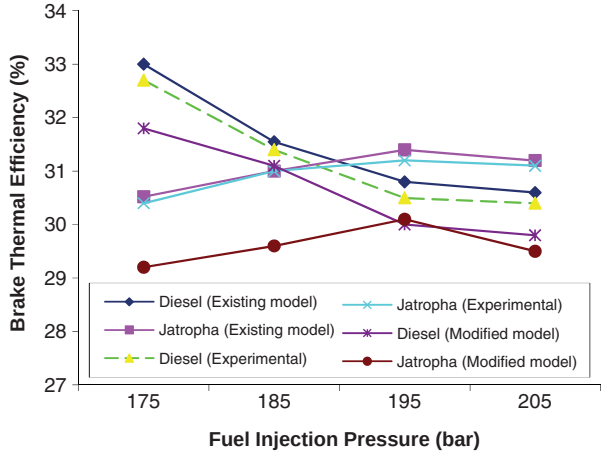

Figure 12. BTE *vs*. injection pressure at speed 1000 rpm, 80% of full load and 20° static injection point (BTDC).

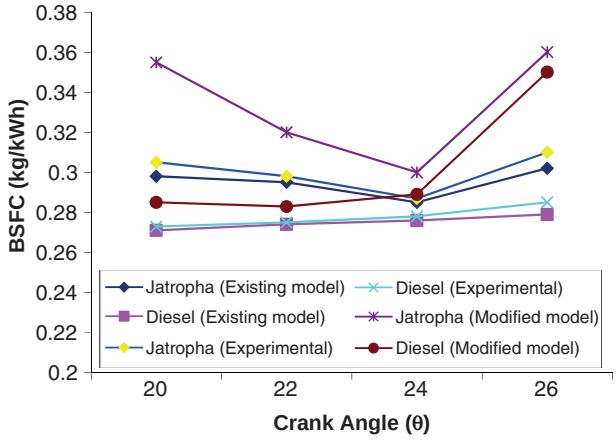

Figure 13. BSFC *vs*. crank angle (BTDC) at speed 1000 rpm, 80% of full load and static 175 bar injection pressure.

6.3. *Effect of fuel injection point on BSFC*

The variation of BSFC keeping fuel injection pressure constant with varying fuel injection point is shown in Figure 13. It has been noticed that the BSFC for diesel is lower than the Jatropha oil operation. However, with the advantages of high operating temperature and the presence of the oxygen molecule in the Jatropha oil, which lowers the calorific value, also has low viscosity, viscosity, CN, and high surface tension result in all together effective combustion characteristics. It can also be seen that the BSFC of the engine with the diesel fuel started increasing whenever the operating point advances. But in the case of Jatropha oil, as the fuel injection angle advances from 20° BTDC to 24° BTDC, it shows a decreasing pattern. When we further advance from 24°, it shows a rising trend. This correlates with BTE trends with change in fuel injection point (Prasath, Tamilporai, and Shabir Mohd 2010).

6.4. *Effect of fuel injection pressure on BSFC*

The effect of the fuel injection pressure keeping the angle constant is plotted in Figure 14. The engine BSFC with diesel fuel increases continuously when the fuel injection pressure increases above 175 bar. But in case of Jatropha oil, BSFC initially started decreasing up to 195 bar and for a further increase in pressure its goes up. Lower viscous fuel breaks into lighter fuel particles at the end of fuel injection which increases atomisation and leads to better combustion. In contrast, higher viscous fuels increase the mixture momentum due to the heavier fuel particle size. This reduces the combustion efficiency of Jatropha oil than diesel. But in contrast, higher combustion efficiency can be obtained for Jatropha oil than diesel engine (Pramanik 2003). The increased mixture momentum and penetration depth are responsible for this improvement, which can be achieved by increasing the fuel injection pressure.

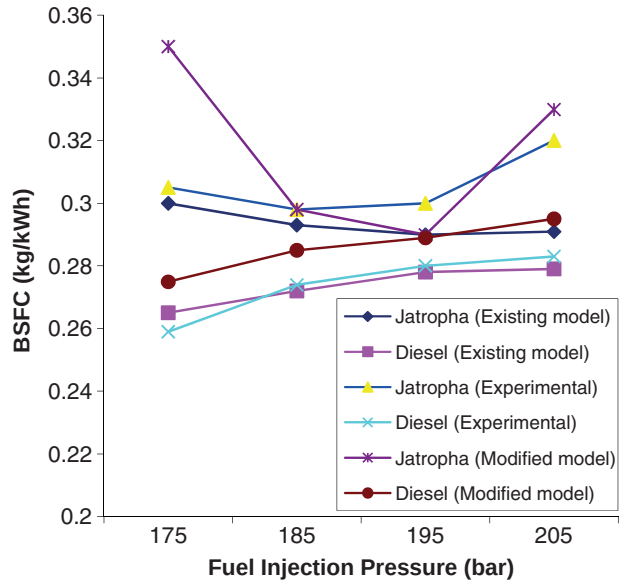

Figure 14. BSFC *vs*. injection pressure at speed 1000 rpm, 80% of full load and 20° static injection point BTDC.

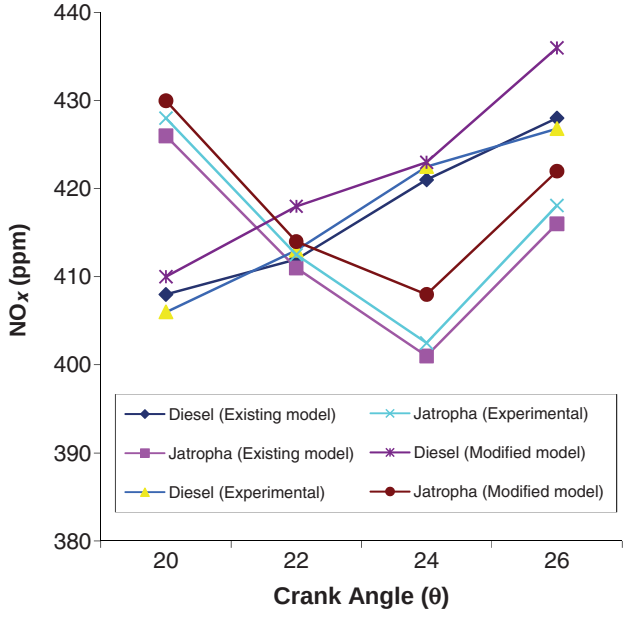

Figure 15. NO_x emission *vs*. crank angle (BTDC) at speed 1000 rpm, 80% of full load and static 175 bar injection pressure.

6.5. *Effect of fuel injection point on NO_x emission*

It is important to consider NO_x as one of the major pollutant and emission concerns. When the combustion temperature is decreased, the emission of NO_x is reduced but the smoke and particulate emission increase. By retarding the injection timing, the temperature inside the combustion chamber decreases and therefore a reduction in the NO_x emission can obtained. Figure 15 represents the trend of fuel injection point variation on NO_x emission keeping the fuel injection pressure constant. This trend shows the continuous increase in the NO_x with diesel fuel as the angle of fuel injection

advances from 20° BTDC. This increased NO_x emission is due to the increase in peak cylinder pressure and temperature as the combustion occurs earlier in the cycle and more heat is released before and around the TDC. The charge elements which burns early in the cycle are subjected to higher temperature and pressure with the advancement in peak timing and remains at high temperatures for a longer period. These early burn elements contribute most to the NO_x formation and hence higher NO_x formation rates result with advanced ignition timing. The NO_x emission for Jatropha oil decreases with advanced angle of fuel injection up to 24° BTDC, but it started increasing with further increase. This reverse behaviour of diesel and Jatropha oil in NO_x emission by varying the point of fuel injection may be because the established combustion process in Jatropha oil might be still later than the diesel fuel. This consequences of late combustion could be due to the low temperature even little beyond the TDC point. This indicates that the combustion efficiency may improve in the case of Jatropha oil as the fuel injection angle advances. The inverse result beyond 24° BTDC may be due to the possibility of engine knocking and erratic behaviour. It was remarkable that the NO_x emission at the operating point (24° BTDC, 195 bar) for Jatropha oil (330 ppm) was even less than the NO_x emission of diesel (360 ppm) at rated operating point (20° BTDC, 175 bar). The predicted trend by this model is very close to the experimental analysis carried out by previous researchers (Lavoie, Heywood, and Keck 1970; Parlak et al. 2005).

6.6. *Effect of the fuel injection pressure on NO_x emission*

From Figure 16, it can be shown that the NO_x emission in the case of diesel fuel increases as the fuel injection pressure increases from 175 bar keeping constant the point of fuel injection. But this trend was reversed when the pressure was further increased from 195 bar. This may be due to the fact that peak pressure and temperature are very close to TDC or even in some cases after TDC which result in exposing the NO_x for very small time periods to the excess air available for the formation of NO_x. The reverse effect on engine beyond the injection pressure of 195 bar might be due to the possibility of engine knocking and erratic behaviour of the engine. In the case of Jatropha oil, it is much more than diesel fuel at 175 bar. But it reduces up to 195 bar and then starts to increase with further rise in pressure (Lavoie, Heywood, and Keck 1970).

6.7. *Comparison of numerical and experimental results*

The BTE of the CI engine fuelled by diesel, Jatropha oil (preheated) and Jatropha oil (unheated) is compared with that obtained from the theoretical model as shown in Figure 17. The BTE of the diesel engine is slightly higher compared with the preheated Jatropha oil-fuelled engine. The BTE of the engine decreases with the use of unheated

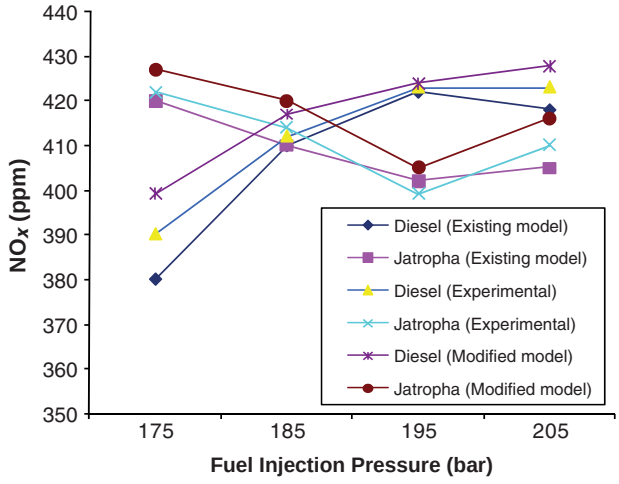

Figure 16. NO_x emission *vs*. injection pressure at speed 1000 rpm, 80% of full load and 20° static injection point BTDC.

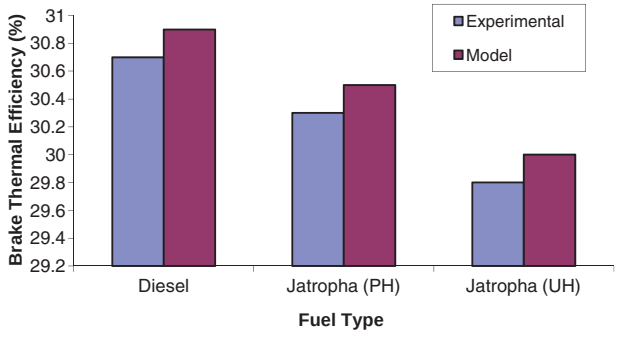

Figure 17. Comparison of BTE.

Jatropha oil. The calorific value of the Jatropha oil is lower than (about 14%) that of diesel because of the presence of oxygen in its molecule. Hence, the BTE of Jatropha oil- (unheated) fuelled engine is lower as compared with that of diesel-fuelled engine. The variation in experimental and theoretical results may be due to the fact that in the theoretical model homogeneous mixture with complete combustion is assumed. But in general, it is difficult to attain complete combustion. Despite the simplification resulting from the assumed hypothesis and empirical relations, the developed simulation proved to be reliable and adequate for the proposed objectives.

6.8. *Validation of the model*

To validate the model, a comparison is given in the present work between the results obtained from the simulation model and the ones obtained from an experimental investigation conducted by me at the University of Petroleum and Energy Studies, Dehradun. The coincidence between calculated and experimental values is good, verifying the accuracy of the simulation model. The values obtained from the proposed model and the detailed one are practically the same for all test conditions examined. The basic data of the

Table 4. Calculations of χ^2 test.

Observed value (O_i) %	30.7	29.8	27.5	28.3	26.2
Expected value (E_i) %	31.7	28.5	30.8	27.5	27.5
$(O_i - E_i)$	−1	1.3	−3.3	0.8	−1.3
$(O_i - E_i)^2$	1	1.69	10.89	0.64	1.69
$(O_i - E_i)^2/E_i$	0.03	0.059	0.35	0.023	0.061

engine are given in Table 2. Furthermore, in order to validate the model against the existing sophisticated models and to find the level of significance in the case of diesel fuel BTE, a χ^2 test is performed which as shown below.

6.8.1. χ^2 test

χ^2 test enables us to ascertain how well the theoretical distribution fits into the empirical distribution. If the calculated value of χ^2 is less than the tabular value at a specified level (generally 5%) of significance, the fit is considered to be good. If the calculated value of χ^2 is greater than the tabular value, the fit is considered to be poor. Calculation of χ^2 is shown in Table 4.

$$\chi^2 = \Sigma\left[\frac{(O_i - E_i)^2}{E_i}\right] = 0.523.$$

Tabular value of χ^2 at 5% level of significance for $n - 1 = 4$ is 7.815.

So $\chi^2_{0.05} = 7.815$. Since the calculated value of χ^2 is less than that of the tabulated value. So, theoretical results support the experimental results.

7. Conclusions

A diesel engine cycle simulation model is modified for predicting the performance of a single-cylinder four-stroke diesel engine fuelled by diesel and Jatropha. The BTE, BSFC and NO_x emission predicted by the model under varying fuel injection pressures and fuel injection point conditions for diesel and Jatropha fuels are analysed and the following conclusions are made based on the results obtained.

(1) With advancing crank angle and increasing fuel injection pressure, the BTE decreases and BSFC increases for diesel fuel and the reverse behaviour has been observed in the case of Jatropha oil up to a limit.
(2) The efficiency of the engine with Jatropha oil improved from 31.0% to 34.8%, which was found to be 1.8 % higher than the diesel fuel. The BSFC was reduced from 0.30 to 0.26 kg/kWh.
(3) NO_x emission on varying fuel injection pressures shows that the emission characteristics improve as the fuel injection pressure is increased from 175 to 195 bar. The emission at operating point (24° BTDC, 195 bar) for Jatropha oil (330 ppm) was even less than the NO_x emission of diesel (360 ppm) at rated operating point (20° BTDC, 175 bar).

The predicted results are compared with the experimental results of the engine fuelled by diesel, Jatropha (PH) and Jatropha (UH). The model predicts that the engine performance characteristics are in closer approximation to that of the experimental results. Hence, it is concluded that this model can be used for the prediction of the performance characteristics of the CI engine fuelled by any hydrocarbon fuel.

Nomenclature

A_n	cross-sectional area of nozzle (m^2)
d	cylinder bore (m)
k	thermal conductivity (W/m K)
L	connecting rod length (m)
l	stroke length (m)
m	mass of the mixture (air + fuel) contained in the combustion chamber (kg)
N	engine speed (rpm)
P	cylinder pressure (Pa)
Q	heat energy (J)
R	universal gas constant (kJ/mol K)
Re	Reynolds's number (dimensionless)
T	temperature (°C)
V	instantaneous cylinder volume (m^3)
V_p	mean piston speed (m/s)
V_Θ	volume at any crank angle (m^3)
V_c	clearance volume (m^3)

Greek

θ	crank angle (degree)
$\Delta\theta$	computational step (°CA)
ΔP	pressure difference (pascal)
ρ	density (kg/m^3)
φ	fuel air equivalence ratio (dimensionless)
ν	kinematic viscosity (m^2/s)
σ	surface tension of fuel (N/m)
γ	specific heat ratio (dimensionless)
μ	dynamic viscosity (kg/m s)

Subscripts

a	air
b	burned zone
c	carbon
com	combustion
f	fuel
h	hydrogen
inj	fuel injection
min	minimum

n species number, or nozzle hole
o oxygen
p piston
u unburned zone
w wall
0 initial value
1 state at the beginning of time step
2 state at the end of time step

References

Balat, M., and H. Balat. 2008. "A Critical Review of Bio-diesel as a Vehicular Fuel." *Energy Conversion and Management* 49: 2727–2741.

Banapurmath, N. R., P. G. Tewari, and R. S. Hosmath. 2008. "Performance and Emission Characteristics of a DI Compression Ignition Engine Operated on Hongue, Jatropha and Sesame Oil Methyl Esters." *Renewable Energy* 33: 1982–1988.

Barnwal, B. K., and M. P. Sharma. 2005. "Prospects of Biodiesel Production from Vegetable Oils in India." *Renewable and Sustainable Energy Reviews* 9: 363–378.

Benson, R. S., and N. D. Whitehouse. 1979. *Internal Combustion Engines*. Oxford: Pergamon.

Bibic, D., I. Filipovic, A. Hribernik, and B. Pikula. 2008. "Investigation into the Effect of Different Fuels on Ignition Delay of M Type Diesel Combustion Process." *Thermal Science* 12 (1): 103–114.

Ferguson, C. R. 1986. *Internal Combustion Engines*. New York: Wiley.

Ganapathy, T., K. Murugesan, and R. P. Gakkhar. 2009. "Performance Optimization of Jatropha Biodiesel Engine Model Using Taguchi Approach." *Applied Energy* 86: 2476–2486.

Ganesan, V. 2000. *Computer Simulation of Compression Ignition Engines*. Hyderabad: University Press Ltd. (India).

Gogai, T. K., and D. C. Baruch. 2010. A cycle simulation model for predicting the performance of a diesel engine fuelled by diesel and biodiesel blends. *Energy* 35: 1317–1323.

Heywood, J. B. 1988. *Internal Combustion Engine Fundamentals*. New York: McGraw-Hill.

Lavoie, G. A., J. B. Heywood, and J. C. Keck. 1970. "Experimental and Theoretical Study of Nitric Oxide Formation in Internal Combustion Engines." *Combustion Science Technology* 1: 313–326.

Parlak, A., H. Yasar, C. Hosimoglu, and A. Kolip. 2005. "The Effects of Injection Timing on NO_x Emissions of a Low Heat Rejection Indirect Diesel Injection Engine." *Applied Thermal Engineering* 25: 3042–3052.

Pramanik, K. 2003. "Properties and Use of Jatropha Curcas Oil and Diesel Fuel Blends in Compression Ignition Engine." *Renewable Energy* 28: 239–248.

Prasath, B. R., P. Tamilporai, and F. Shabir Mohd. 2010. "Theoretical Modeling and Experimental Study of Combustion and Performance Characteristics of Biodiesel in Turbocharged Low Heat Rejection D.I Diesel Engine." *World Academy of Science*, *Engineering and Technology* 61: 435–445.

Quintero, H. F., C. A. Romero, and L. V. Vanegas Useche. 2007. "Thermodynamic and Dynamic Analysis of an Internal Combustion Engine with a Noncircular-Gear Based Modified Crank-Slider Mechanism." 12th IFToMM World Congress, Besançon, France.

Rakopoulos, C. D., K. A. Antonopoulos, and D. C. Rakopoulos. 2007. "Development and Application of Multi-Zone Model for Combustion and Pollutants Formation in Direct Injection Diesel Engine Running with Vegetable Oil or Its Bio-Diesel." *Energy Conversion and Management* 48: 1881–1901.

Rakopoulos, C. D., D. T. Hountalas, G. N. Taklis, and E. I. Tzanos. 1995. "Analysis of Combustion and Pollutants Formation in a Direct Injection Diesel Engine Using a Multi-Zone Model." *Energy Research* 19: 63–88.

Rakopoulos, C. D., D. C. Rakopoulos, E. G. Giakoumis, and D. C. Kyritsis. 2004. "Validation and Sensitivity Analysis of a Two Zone Diesel Engine Model for Combustion and Emissions Prediction." *Energy Conversion and Management* 45: 1471–1495.

Ramadhas, A. S., S. Jayaraj, C. Muraleedharan. 2006. "Theoretical Modeling and Experimental Studies on Biodiesel-Fueled Engine." *Renewable Energy* 31: 1813–1826.

Senthil Kumar, M., A. Ramesh, and B. Nagalingam. 2003. "An Experimental Comparison of Methods to Use Methanol and Jatropha Oil in a Compression Ignition Engine." *Biomass and Bioenergy* 25: 309–318.

Zweiri, Y. H., J. F. Whidborne, and L. D. Seneviratne. 2001. "Detailed Analytical Model of a Single-Cylinder Diesel Engine in the Crank Angle Domain." *Journal of Automobile Engineering* 215: 1197–1216.